Anomaly Detection in Directed Energy Deposition: A Comparative Study of Supervised and Unsupervised Machine Learning Algorithms

Berke Ayyıldızlı, Beyza Balota, Kerem Tatari, Shawqi Mohammed Farea and Mustafa Unel Faculty of Engineering and Natural Sciences, Sabancı University, Istanbul, Turkey

Keywords: Directed Energy Deposition (DED), Thermal Imaging, Anomaly Detection, Supervised Learning,

Unsupervised Learning, Machine Learning.

Abstract: Directed Energy Deposition (DED) is a promising additive manufacturing technology increasingly utilized in

critical industries such as aerospace and biomedical engineering for fabricating complex metal components. However, ensuring the structural integrity of DED-fabricated parts remains a significant challenge due to the emergence of in-process defects. To address this, we propose a comprehensive anomaly detection framework that leverages in-situ thermal imaging of the melt pool for defect identification. Our approach encompasses both supervised and unsupervised machine learning techniques to capture diverse defect patterns and accommodate varying levels of labeled data availability. Supervised methods—including ensemble classifiers and deep neural networks—are employed to learn from annotated thermal data, while unsupervised methods, such as autoencoders and clustering algorithms, are used to detect anomalies in unlabeled scenarios and uncover previously unknown defect patterns. The pipeline incorporates essential preprocessing techniques—such as feature extraction, normalization, and class rebalancing—to enhance model robustness. Experimental evaluations offer a detailed comparison between the supervised classifiers and unsupervised methods. Notably the supervised elegification based framework achieved high performance in detecting paradigm. Notably the supervised elegification based framework achieved high performance in detecting paradigm.

tably, the supervised classification-based framework achieved high performance in detecting porosity-related anomalies, with an F1 score of up to 0.88 and accuracy reaching 99%.

1 INTRODUCTION

Directed Energy Deposition (DED) is a key additive manufacturing process that enables the fabrication and repair of complex metal components layer by layer using a focused energy source. Its flexibility makes it particularly well-suited for high-stakes industries such as aerospace, healthcare, and automotive manufacturing, where mechanical integrity is essential for ensuring safe and reliable operation (Dass and Moridi, 2019; Li et al., 2023). Compared to traditional manufacturing techniques, DED facilitates the creation of intricate geometries and enables localized repairs, offering significant advantages in both design flexibility and material efficiency.

Despite these benefits, DED processes are prone to critical in-process defects—most notably porosity, lack of fusion, and cracking—that can degrade the performance and service life of the fabricated parts (Tang et al., 2022). Early identification of such defects is essential, especially in applications where structural failure could have catastrophic con-

sequences. Conventional inspection techniques, including manual review and post-process nondestructive evaluation methods such as X-ray Computed Tomography (XCT), are limited by their inability to provide real-time feedback and often require significant time and resources (Tang et al., 2022; Herzog et al., 2024). Additionally, fixed-threshold and rule-based monitoring methods fall short in capturing the complex and transient thermal patterns present in DED processes (Herzog et al., 2024).

In contrast, machine learning (ML) has emerged as a promising approach for real-time, non-invasive defect detection, offering the ability to learn complex and nonlinear relationships from high-dimensional data sources such as thermal imagery (Gaja and Liou, 2018). These data-driven methods can generalize across subtle patterns that are difficult to capture using deterministic thresholds or handcrafted rules, making them ideal for DED monitoring. In the existing literature, a variety of supervised ML classifiers have been employed for defect detection, including discriminant analysis, support vector machines, and en-

semble methods (Khanzadeh et al., 2018), as well as deep neural network architectures (Patil et al., 2023). In addition, unsupervised learning techniques—such as self-organizing maps (SOM), K-means clustering, and Density-Based Spatial Clustering of Applications with Noise (DBSCAN)—have also been explored for identifying anomalies in thermal data during the DED process (Taheri et al., 2019; García-Moreno, 2019; Farea et al., 2024).

However, several research gaps remain unaddressed. First, there is a lack of comparative studies that rigorously evaluate supervised and unsupervised ML methods side-by-side for DED defect detection, especially in terms of robustness under realworld conditions. Most prior works tend to focus exclusively on one paradigm without assessing the strengths and limitations of both. Second, threshold selection in anomaly detection—particularly for unsupervised methods like autoencoders—often lacks standardized or domain-specific criteria, making it difficult to generalize results across datasets and applications. Lastly, practical concerns such as extreme class imbalance, data quality issues, and interpretability are frequently underexplored, despite their significant impact on real-world deployment.

In this study, we introduce a comprehensive framework that leverages both supervised and unsupervised ML techniques to detect porosity-related defects in DED using thermal image data. The unsupervised models include autoencoders and DBSCAN, whilst the supervised models include Random Forest, Extreme Gradient Boosting (XGBoost), and Convolutional Neural Networks (CNNs). These models are tested on a dataset comprising 1,564 thermal images of the melt pool, where only 4.5% of images contain porosity-related defects (Zamiela et al., 2023). This severe class imbalance introduces modeling challenges and necessitates preprocessing strategies tailored to noisy, sparse, and imbalanced data. A preprocessing pipeline was implemented to overcome these limitations, including outlier removal, data imputation, normalization, and class rebalancing. Furthermore, feature extraction was used to support interpretable models and reduce input dimensionality. Extracted features include statistical descriptors of the melt pool's thermal distribution—such as mean, standard deviation, skewness, and interquartile range—which have been shown in prior research to correlate with melt pool quality and porosity formation (García-Moreno, 2019).

This work offers a comparative study of ML methods for DED defect detection, with an emphasis on practical issues such as data imbalance, preprocessing complexity, thresholding strategies, and model

interpretability. By combining domain knowledge with modern ML techniques, the proposed framework aims to advance real-time defect detection in additive manufacturing. Ultimately, the results contribute to the goal of establishing DED as a robust and reliable process for safety-critical industrial applications.

2 METHODOLOGY

2.1 Preprocessing Pipeline

Due to inconsistencies and noise present in the raw thermal image data, a robust preprocessing pipeline was implemented to prepare model-ready inputs and enhance the performance of both supervised and unsupervised learning models.

Some images in the dataset contain zero-valued pixels and/or pixels with missing values. The values of these pixels were imputed using the mean of their respective columns within each image. Then, the thermal data underwent min-max normalization, scaling pixel values to the range of [0, 1]. This normalization step was crucial for stabilizing gradient-based optimizers in neural network training and ensuring consistency and comparability across ML models.

For the shallow models, feature extraction was employed to reduce dimensionality and enhance interpretability. Each thermal image was transformed into a structured feature vector comprising 11 statistical descriptors: minimum (Min_Temp), maximum (Max_Temp), mean (Mean_Temp), standard deviation (Std_Temp), median (Median_Temp), first quartile (Q1), third quartile (Q3), interquartile range (IQR), skewness, kurtosis, and peak temperature pixel (High_Temp_Pixels). These features summarize the spatial and statistical properties of the melt pool temperature distribution, providing a compact and informative input format for training the supervised tree-based classifiers—the Random Forest and XGBoost classifiers.

Considering the inherent imbalance in the dataset, the Synthetic Minority Oversampling Technique (SMOTE) was employed during the training of the supervised models. SMOTE generates synthetic minority class samples by interpolating between existing anomalous instances, mitigating classification bias, and improving the defect detection recall.

Collectively, these preprocessing strategies ensured the dataset's compatibility and consistency across diverse ML models, ultimately enhancing the effectiveness and interpretability of the anomaly detection framework.

2.2 Supervised ML Models

2.2.1 Ensemble Tree-Based Models

The ensemble tree-based models include two effective classifiers as follows:

Random Forest: It is an ensemble ML algorithm that combines multiple decision trees to deliver robust predictions through majority voting (Rigatti, 2017). Random forests are particularly effective in handling high-dimensional data, reducing overfitting, and providing feature importance insights, making them a preferable choice for anomaly detection in DED processes using thermal image-derived features.

XGBoost: It is an advanced gradient boosting framework that builds upon traditional tree-based ensemble methods by employing iterative training of shallow decision trees (Chen and Guestrin, 2016). XGBoost is especially renowned for its performance on structured, tabular datasets and its inherent robustness in managing class imbalance, sparse features, and noisy data, making it particularly suitable for anomaly detection in DED processes.

Both classifiers were configured and fine-tuned to achieve optimal performance while ensuring generalizability. Through preliminary experimentation and cross-validation, the hyperparameters were selected according to Table 1, ensuring the best compromise between predictive accuracy and model simplicity. The random state was set at 42 for reproducibility of experimental results.

For both classifiers, a structured feature vector comprising 11 statistical features extracted from the thermal images was used as input. The dataset was divided into training and test sets using a stratified 70%-30% split, preserving the original class distribution within each subset. The SMOTE algorithm was then applied solely to the training set to avoid data leakage and realistically simulate practical scenarios, resulting in balanced class proportions that enhance the classifier's sensitivity to anomalies.

By leveraging carefully extracted statistical features, robust oversampling techniques, and thorough hyperparameter tuning, these supervised approaches significantly enhances the defect detection process, as can be noticed in Section 3.

Table 1: Hyperparameters of Random Forest and XGBoost.

Random Forest		XGBoost		
Number of Estimators	100	Number of Estimators	100	
Max. Depth	5	Max. Depth	3	
Min. Samples per Split	5	L2 Regularization	1	
Min. Samples per Leaf	2	L1 Regularization	0.5	

Lastly, one of the inherent key strengths of Random Forest and XGBoost lies in their transparency regarding feature importance, allowing practitioners to directly interpret and understand critical features impacting anomaly detection outcomes. This interpretability is particularly beneficial for manufacturing engineers and quality analysts in pinpointing key indicators of defects in real-world DED processes.

2.2.2 Convolutional Neural Network (CNN)

CNNs are a subclass of deep learning models, particularly effective for spatial data such as images. In this study, CNNs were utilized in a supervised learning context to directly classify thermal images as either defective or non-defective.

After preprocessing, the dataset was split into training and test sets with an 70%-30% stratified split to preserve class distribution. To address the highly imbalanced nature of the dataset, SMOTE was applied to the training set. Since SMOTE requires 2D inputs, training images were first flattened, oversampled, and reshaped back to their original shape.

The CNN architecture consisted of the following layers:

- Conv2D (16 filters) with ReLU activation and a 3 × 3 kernel, followed by a maximum pooling layer.
- Conv2D (32 filters) with ReLU activation and a 3 × 3 kernel, followed by a maximum pooling layer
- Flatten layer to convert spatial features into a dense vector.
- **Dropout layer (rate = 0.3)** to prevent overfitting.
- Dense layer (64 units) with ReLU activation.
- Output layer (1 unit) with sigmoid activation for binary classification.

The model was compiled with the Adam optimizer (learning rate = 0.001), using the binary crossentropy loss. The network was trained for 10 epochs with a batch size of 16, using 20% of the training data as a validation set.

2.3 Unsupervised ML Models

2.3.1 Autoencoder

Autoencoders are a class of artificial neural networks primarily used for unsupervised learning and anomaly detection. They are designed to learn compressed, low-dimensional representations of the input data and subsequently reconstruct the input from this encoding. Deviations between the input and reconstructed

output serve as a basis for identifying anomalous instances. Instances with high reconstruction errors are considered potential anomalies, as they deviate from the learned patterns of normal data (Zhou and Paffenroth, 2017). Since autoencoders are trained solely to reproduce their input, they do not require labeled data, making them inherently suitable for unsupervised anomaly detection.

The model implemented in this study consists of three primary layers: an input, encoding layer, and decoding layer. The input layer accepts flattened vectors of the thermal images. The encoding layer contains 64 neurons, strategically selected through empirical testing to ensure sufficient information retention without overfitting. This layer employs the ReLU activation function because of its efficacy in handling continuous numeric data and mitigating issues such as vanishing gradients. The decoding layer mirrors the dimensionality of the input layer and uses a sigmoid activation function to produce output values within a normalized range of 0 to 1, ensuring compatibility with the scaled thermal image data.

The autoencoder was trained using the entire dataset of preprocessed thermal images, consisting of 1,564 frames, each normalized to manage pixel value disparities. The training regime consisted of 50 epochs with a batch size of 16, determined through preliminary experimentation to balance training performance and computational efficiency. During training, input data points were continuously reconstructed, using the Adam optimizer to minimize the mean square error (MSE) loss between the original and reconstructed frames.

After training, anomaly detection was performed by evaluating the reconstruction error for each thermal frame. The underlying hypothesis is that anomalous frames, characterized by porosity or structural defects, inherently deviate significantly from normal thermal patterns, resulting in a higher reconstruction error. To systematically identify anomalies, two distinct thresholds based on the percentile distribution of reconstruction errors were established:

- 95th Percentile Threshold: Frames with MSE above the 95th percentile were labeled anomalous.
- **99th Percentile Threshold:** A more conservative approach, identifying only the extreme deviations by setting a threshold at the 99th percentile.

This dual-threshold strategy allowed a nuanced analysis of detection sensitivity and specificity, providing insights into the optimal balance for practical anomaly detection within industrial contexts. Overall, the autoencoder-based anomaly detection methodol-

ogy outlined provides a robust, unsupervised framework adaptable for monitoring DED processes, offering a valuable alternative when labeled data is scarce or expensive to obtain.

2.3.2 DBSCAN

It is a density-based clustering algorithm widely used in unsupervised anomaly detection tasks. Unlike traditional clustering algorithms, DBSCAN does not require a predefined number of clusters; instead, it identifies clusters based on the density of data points, classifying points in low-density regions as anomalies (Deng, 2020). Given the high-dimensional nature of the thermal images, dimensionality reduction was critical for the effective application of DBSCAN. Principal Component Analysis (PCA) was employed to reduce the dimensionality of the input thermal images to 50 principal components (Hemanth, 2020). This transformation significantly decreased computational complexity, improved clustering efficiency, and enhanced the clarity of density-based clusters.

Nonetheless, the optimal parameter selection is essential for DBSCAN performance. The algorithm primarily depends on two parameters: the neighborhood radius (ϵ) and the minimum number of points required to form a dense region (min_samples). To determine the optimal ε value, a k-distance heuristic method was utilized, as displayed in Figure 1. Specifically, distances to the 5th nearest neighbor for each data point were calculated, sorted, and plotted to identify an elbow point—representing an optimal balance between overly fragmented clusters (too small $\boldsymbol{\epsilon})$ and merged clusters (too large ε). Based on this heuristic, the ε value was set to 7.7, while the min_samples parameter was set to 5 (see Figure 1). This configuration provided an effective balance, ensuring that densitybased clustering appropriately distinguished anomalies from typical data patterns. With the optimized parameters, DBSCAN clusters the PCA-transformed image data into dense regions, labeling points outside these clusters as anomalies.

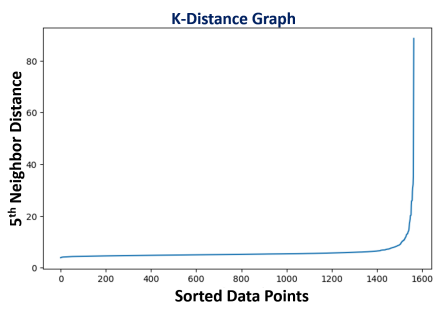


Figure 1: K-Distance graph used for optimal epsilon value selection. The sharp increase (elbow) around 7.7 suggests this as the optimal ϵ value.

3 RESULTS AND DISCUSSION

3.1 Dataset Description

The dataset used in this work (Zamiela et al., 2023) consists of 1,564 thermal images of the melt pool recorded during the fabrication of Ti-6Al-4V thinwalled structures using the OPTOMEC LENSTM 750 system. The thermal images were captured in-process using a Stratonics dual-wavelength pyrometer, which records a top-down view of the melt pool during laser deposition. Each frame consists of a 200×200 pixel thermal image capturing the relative temperature distribution of the melt pool. Binary porosity labels were assigned based on post-process inspection using Nikon XT H225 X-ray Computed Tomography. Only 71 images (about 4.5%) contain porosity-related defects, whilst the remaining 1493 images are defectfree, leading to a significant class imbalance. This remarkable class imbalance poses challenges for model generalization and sensitivity to rare events. Representative defect-free and defective images are shown in Figure 2.

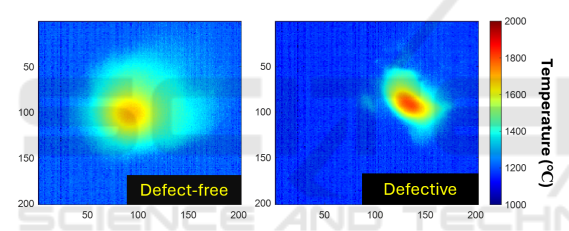


Figure 2: Normal vs defective thermal images.

3.2 Defect Detection Results

The comparative evaluation of the models is presented in Tables 2 and 3, with corresponding confusion matrices shown in Figures 3 and 4. Each model was assessed based on its ability to identify porosity-related anomalies from thermal image data, under the same preprocessing and evaluation.

Among the supervised models, the CNN model exhibited the most favorable performance profile. It achieved the most balanced trade-off between precision and recall, and demonstrated minimal misclassification of both normal and defective instances, as reflected in its confusion matrix. The direct use of image-level data, without handcrafted features, likely contributed to its ability to capture nuanced spatial patterns indicative of structural defects.

The ensemble tree-based models yielded good results, although working with low-dimensional input data compared to CNN. In particular, Random Forest achieved results comparable to CNN with an F1 score

Table 2: Supervised models results.

Model	Precision	Recall	F1-Score	Accuracy
CNN	0.90	0.86	0.88	0.99
Random Forest	0.86	0.86	0.86	0.98
XGBoost	0.89	0.76	0.82	0.98

Table 3: Unsupervised models results.

Model	Precision	Recall	F1-Score	Accuracy
Autoencoder (99th)	0.75	0.17	0.28	0.96
Autoencoder (95th)	0.54	0.61	0.57	0.96
DBSCAN	0.54	0.52	0.53	0.96

of 0.86. It yielded consistently high results across all metrics. The confusion matrix for Random Forest reveals only a small number of false positives and false negatives, underscoring its reliability in practical classification tasks. XGBoost, while slightly behind the other two, remained a competitive model with high precision and moderate recall. Its performance suggests that it is more conservative in detecting anomalies, favoring precision over sensitivity. This behavior can be useful in industrial settings where minimizing false alarms is critical, though it may result in some defective instances being overlooked.

In contrast, the unsupervised models demonstrated a wider range of performance, with substantial variation depending on threshold sensitivity and underlying assumptions. The autoencoder's detection capability was heavily influenced by the selected percentile threshold. At the 95th percentile, it captured a larger portion of true anomalies but also introduced more false positives. The 99th percentile threshold, being more conservative, reduced false positives at the expense of significantly lower recall. This tradeoff is clearly reflected in the differences between the two confusion matrices in Figure 4.

DBSCAN, as a clustering-based method, struggled to consistently distinguish defective instances from the background class (normal class). Its detection capability was less focused, and it tended to misclassify both normal and anomalous samples. Despite dimensionality reduction via PCA and careful parameter tuning, DBSCAN's density-based assumptions proved less effective in this context, where anomalies are subtle and highly variable.

When comparing the two learning paradigms, supervised models consistently outperformed their unsupervised counterparts across all evaluation metrics. The availability of labeled data, combined with class rebalancing techniques such as SMOTE, enabled supervised classifiers to learn more discriminative decision boundaries. Crucially, these models are explicitly trained and optimized to classify thermal images as either normal or anomalous. In contrast, unsupervised models are typically designed for auxiliary

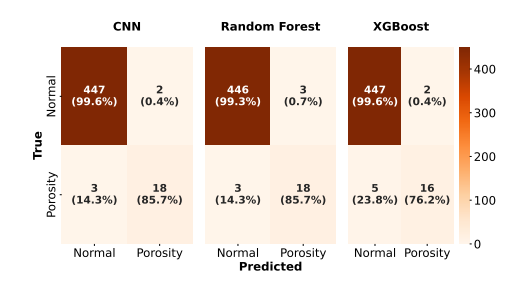


Figure 3: Confusion matrices of the supervised models.

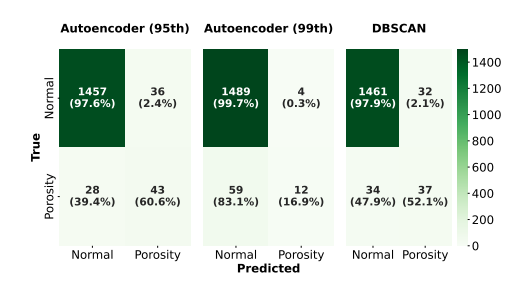


Figure 4: Confusion matrices of the unsupervised models.

tasks, such as input reconstruction or density estimation, that are not directly aligned with classification objectives. This mismatch limits their sensitivity to subtle, class-specific patterns, particularly in imbalanced datasets. Although autoencoders provided a flexible and scalable detection framework, their performance was highly dependent on threshold selection. Similarly, DBSCAN lacked the granularity necessary for fine-grained anomaly identification. Collectively, these findings underscore the advantages of supervised learning when labeled data is available, while also highlighting the potential of unsupervised methods as complementary tools—provided they are carefully tuned for the task.

3.3 Feature Analysis

Feature-level analysis revealed several insights into model behavior and predictive performance. To better understand the relationships among input features, a Pearson correlation test was conducted. The correlation matrix, shown in Figure 5, indicates strong collinearity among central tendency features such as *Mean_Temp*, *Median_Temp*, *Q1*, and *Q3*, suggesting redundancy in the thermal distribution representation. In contrast, features like *Skewness*, *Kurtosis*, and *IQR* demonstrated lower correlation with others, implying they provide orthogonal, potentially more informative cues for anomaly detection.

The feature importance rankings derived from supervised models further validate the relevance of specific features. The importance plots for Random Forest and XGBoost are provided in Figure 6a and 6b, respectively. Both Random Forest and XGBoost consistently prioritized dispersion metrics—*IQR* and *Std_Temp*—as the most influential attributes in distinguishing between normal and defective samples. This aligns with the observation that defective frames often display abrupt changes in temperature variance, which are effectively captured by interquartile spread and standard deviation.

Interestingly, while *Min_Temp* and *Median_Temp* appeared highly correlated in the correlation matrix, their respective importances varied between models—suggesting that although correlated, they do not necessarily provide equivalent discriminative value. This underscores the benefit of ensemble-based feature evaluation, where subtle nonlinear relationships are accounted for during tree construction.

Altogether, the correlation and feature importance analyses offer actionable insights for dimensionality reduction, feature selection, and interpretability. They confirm that a subset of carefully engineered features—particularly those reflecting distribution shape and spread—can effectively support robust classification, even in imbalanced anomaly detection settings.

3.4 Final Remarks

Learning Paradigm: Supervised models clearly benefited from labeled data and class rebalancing techniques, enabling them to achieve higher and more consistent detection accuracy. However, this advantage comes at the cost of increased data annotation effort and reduced flexibility. In industrial settings where defect annotation is costly or infeasible at scale, the reliance of supervised models on labeled datasets may limit their broader applicability. In contrast, unsupervised models offered greater flexibility by operating without labeled defect data, making them appealing for anomaly detection in exploratory or early-stage quality monitoring systems.

Threshold Sensitivity and Stability: While autoencoders provided a scalable and adaptable framework capable of learning general thermal patterns, their effectiveness was tightly coupled to the choice of reconstruction error threshold. This introduces subjectivity and leads to performance tradeoffs—particularly between recall and false-positive rates. Similarly, DBSCAN was highly sensitive to parameter selection (ε and *min_samples*) and struggled with the subtle and highly variable defect patterns typical of DED processes.

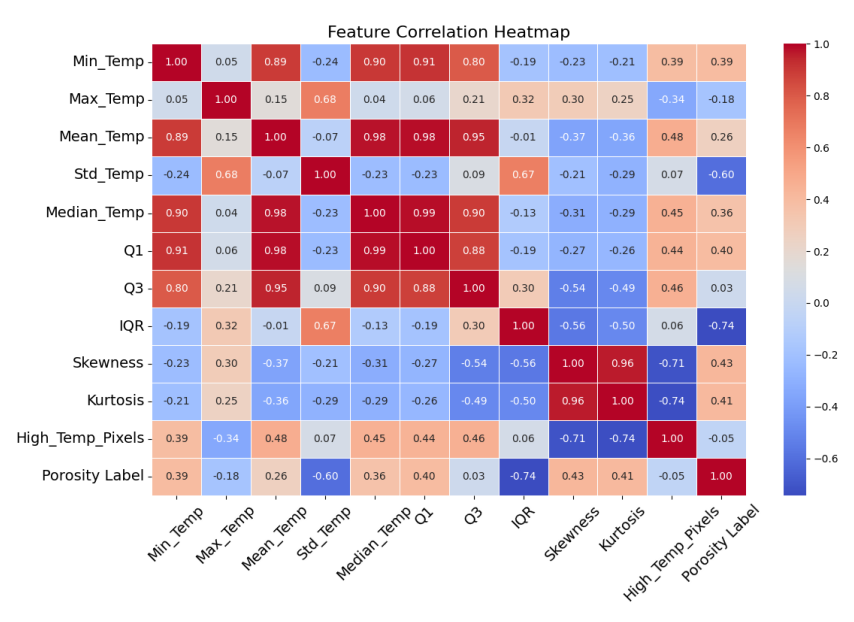
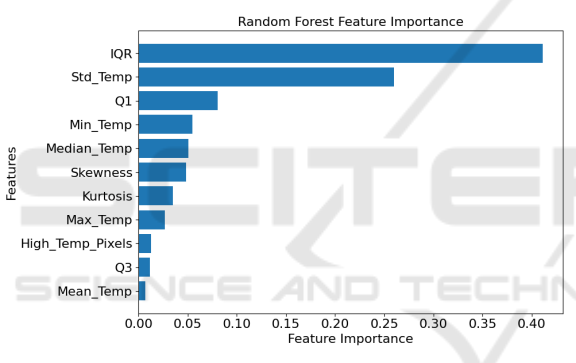


Figure 5: Feature correlation heatmap among extracted statistical features.



(a) Random Forest

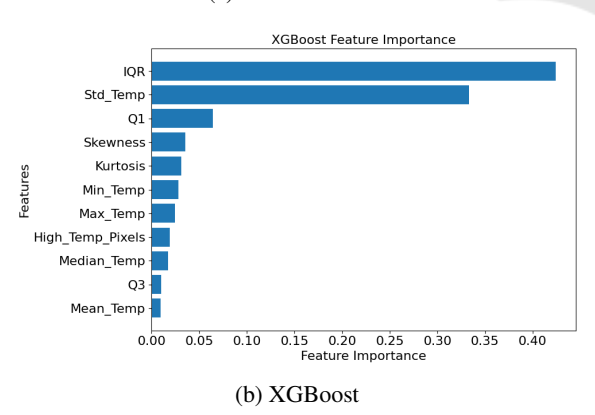


Figure 6: Feature importance plot from the ensemble treebased models.

Interpretability and Practical Transparency: From an interpretability standpoint, the supervised tree-based models—Random Forest and

XGBoost—provided clear advantages. Through feature importance rankings, these models enabled traceable classification decisions and gave practitioners direct insights into which statistical temperature features were most indicative of porosity-related anomalies. This level of transparency is particularly valuable in high-stakes manufacturing environments, where model trustworthiness is critical. On the other hand, although unsupervised models are more adaptable, their decisions are often harder to explain—especially when based on latent encodings or density-based assumptions.

Deployment Considerations: While supervised models deliver stronger performance when sufficient labeled data is available, their deployment requires pre-existing defect annotations and careful data balancing. Unsupervised approaches, however, can be rapidly deployed in dynamic environments with limited prior knowledge, making them better suited for initial system integration or ongoing monitoring. The optimal deployment strategy may involve a hybrid approach—utilizing unsupervised methods for continuous monitoring or early anomaly flagging, followed by supervised refinement when annotated data becomes available.

4 CONCLUSION

This study presents a comprehensive comparison of supervised and unsupervised learning approaches

for anomaly detection in DED processes based on thermal image data, highlighting the respective strengths and limitations of each paradigm. Supervised models—namely, CNN, Random Forest, and XGBoost—consistently outperformed their unsupervised counterparts, benefiting from labeled data, synthetic oversampling via SMOTE, and, for the tree-based models, statistically engineered features. While autoencoders and DBSCAN offered greater flexibility and did not require labeled data, their performance was more sensitive to thresholding and parameter selection.

The results highlight the practicality and reliability of supervised learning in quality-critical applications where labeled datasets are available. However, unsupervised methods remain valuable for early-stage deployment and real-time monitoring scenarios. Moving forward, hybrid frameworks that combine the strengths of both paradigms—starting with unsupervised detection and refining with supervised feedback—offer a promising direction for scalable, interpretable, and robust defect detection in metal additive manufacturing.

REFERENCES

- Chen, T. and Guestrin, C. (2016). XGBoost: A scalable tree boosting system. In *Proceedings of the 22nd ACM SIGKDD International Conference on Knowledge Discovery and Data Mining*, pages 785–794, San Francisco, CA, USA.
- Dass, A. and Moridi, A. (2019). State of the art in directed energy deposition: From additive manufacturing to materials design. *Coatings*, 9(7):418.
- Deng, D. (2020). DBSCAN clustering algorithm based on density. In *Proceedings of the 2020 7th International Forum on Electrical Engineering and Automation (IFEEA)*, pages 100–103, Zhuhai, China.
- Farea, S. M., Unel, M., and Koc, B. (2024). Defect prediction in directed energy deposition using an ensemble of clustering models. In *Proceedings of the 2024 IEEE 22nd International Conference on Industrial Informatics (INDIN)*, pages 1–6.
- Gaja, H. and Liou, F. (2018). Defect classification of laser metal deposition using logistic regression and artificial neural networks for pattern recognition. *Interna*tional Journal of Advanced Manufacturing Technology, 94:315–326.
- García-Moreno, A.-I. (2019). Automatic quantification of porosity using an intelligent classifier. *Interna*tional Journal of Advanced Manufacturing Technology, 105(5):1883–1899.
- Hemanth, D. J. (2020). Dimensionality reduction of production data using PCA and DBSCAN techniques. *International Journal of Scientific Research in Engineering and Development*, 3(6):325–329.

- Herzog, T., Brandt, M., Trinchi, A., et al. (2024). Defect detection by multi-axis infrared process monitoring of laser beam directed energy deposition. *Scientific Re*ports, 14(1):3861.
- Khanzadeh, M., Chowdhury, S., Marufuzzaman, M., Tschopp, M. A., and Bian, L. (2018). Porosity prediction: Supervised-learning of thermal history for direct laser deposition. *Journal of Manufacturing Systems*, 47:69–82.
- Li, S. H., Kumar, P., and Chandra, S. (2023). Directed energy deposition of metals: Processing, microstructures, and mechanical properties. *International Materials Reviews*, 68(1):1–44.
- Patil, D. B., Nigam, A., Mohapatra, S., and Nikam, S. (2023). A deep learning approach to classify and detect defects in the components manufactured by laser directed energy deposition process. *Machines*, 11(9).
- Rigatti, S. J. (2017). Random forests. *Journal of Insurance Medicine*, 47(1):31–39.
- Taheri, H., Koester, L. W., Bigelow, T. A., Faierson, E. J., and Bond, L. J. (2019). In situ additive manufacturing process monitoring with an acoustic technique: clustering performance evaluation using k-means algorithm. *Journal of Manufacturing Science and Engi*neering, 141(4).
- Tang, D., He, X., Wu, B., Wang, X., Wang, T., and Li, Y. (2022). The effect of porosity defects on the mid-cycle fatigue behavior of directed energy deposited Ti-6Al-4V. *Theoretical and Applied Fracture Mechanics*, 118:103296.
- Zamiela, C., Tian, W., Guo, S., and Bian, L. (2023). Thermal-porosity characterization data of additively manufactured Ti–6Al–4V thin-walled structure via laser engineered net shaping. *Data in Brief*, 51:109722.
- Zhou, C. and Paffenroth, R. C. (2017). Anomaly detection with robust deep autoencoders. In *Proceedings of the 23rd ACM SIGKDD International Conference on Knowledge Discovery and Data Mining (KDD)*, pages 665–674.